The Self-Assembly of a Highly Ordered [2]Catenane

Peter R. Ashton,[a] Christopher L. Brown,[a] Ewan J. T. Chrystal,[b] Timothy T. Goodnow,[c] Angel E. Kaifer,[c] Keith P. Parry,[b] Douglas Philp,[a] Alexandra M. Z. Slawin,[d] Neil Spencer,[a] J. Fraser Stoddart[a] and David J. Williams[d]

[a] *Department of Chemistry, The University, Sheffield S3 7HF, UK*
[b] *ICI Agrochemicals, Jealott's Hill Research Station, Bracknell RG12 6EY, UK*
[c] *Department of Chemistry, University of Miami, Coral Gables, Florida 33124, USA*
[d] *Department of Chemistry, Imperial College, London SW7 2AY, UK*

Template-directed synthesis has been used to construct a [2]catenane in which the two molecular components, the cyclobis(paraquat-*p*-phenylene) tetracation and 1,5-dinaphtho-38-crown-10, are found to be ordered non-covalently with respect to each other in both the solid (by X-ray crystallography) and solution (by NMR spectroscopy) states and to influence each other to the extent of establishing electrochemical gradients for the stepwise one electron reductions of the two paraquat units.

In the knowledge (*a*) that 1,5-dinaphtho-44-crown-12 (1/5DN44C12) forms[1] a 1:2 crystalline complex with the Paraquat (PQT^{2+}) dication and (*b*) that 1,5-dimethoxynaphthalene (1/5DMN) can be included[2] within the cavity of the cyclobis(paraquat-*p*-phenylene) tetracation $\mathbf{1}^{4+}$ in a manner[3,4] directly analogous to 1,4-dimethoxybenzene, coupled with (*c*) the fact that bisparaphenylene-34-crown-10 (BPP34C10) can be used[5,6] to template the formation of the [2]catenane $\mathbf{2}^{4+}$, we have extended this philosophy and strategy to the template-directed synthesis (Fig. 1) of a [2]catenane $\mathbf{3}^{4+}$ involving 1,5-dinaphtho-38-crown-10 (1/5DN38C10) and $\mathbf{1}^{4+}$. In addition to describing the preparation (Scheme 1) of this new [2]catenane $\mathbf{3}^{4+}$, we also report (*a*) the FABMS† of $\mathbf{3}\cdot 4PF_6$, (*b*) its single crystal X-ray structure,‡ (*c*) its dynamic ^1H NMR spectroscopic behaviour, and (*d*) its distinctive redox properties.

When the bis(pyridinium) salt[7] $\mathbf{4}\cdot 2PF_6$ (100 mg, 0.14 mmol), 1,4-bis(bromomethyl)benzene **5** (46 mg, 0.17 mmol) and 1/5DN38C10 (100 mg, 0.15 mmol) were stirred in MeCN at room temperature, a deep purple colour was generated within 2 h. After 2 days, the solvent was evaporated off to afford a bright purple solid, which was subjected to column chromatography [SiO_2 : MeOH–NH_4Cl (2 mol dm^{-3}) : $MeNO_2$ (7:2:1)]. The fractions containing the highly coloured product were mixed with a saturated aqueous solution of NH_4PF_6 until no further precipitation occurred. The precipitate was filtered off, dissolved in $MeNO_2$ and then washed with H_2O, before being isolated as a solid residue, which was finally washed successively with H_2O, MeOH and Et_2O to give the pure $\mathbf{3}\cdot 4PF_6$ (129 mg, 51%), m.p. > 280 °C, which was characterised by positive-ion FABMS† in the first instance. Peaks were revealed at *m/z* 1592, 1446 and 1301 corresponding to the loss of one, two and three PF_6 counterions, respectively from $\mathbf{3}\cdot 4PF_6$. Single crystals, suitable for X-ray crystallography, were grown by vapour diffusion of Pr^i_2O into a solution of $\mathbf{3}\cdot 4PF_6$ in MeCN. The X-ray crystal structure (Fig. 2) of $\mathbf{3}^{4+}$ reveals, as in the case of $\mathbf{2}^{4+}$, an interlocked and highly ordered molecular arrangement in which one 1,5-dinaphtho residue is sandwiched between the two bipyridin-

---

† FABMS was carried out on a Kratos MS80RF mass spectrometer (accelerating voltage, 3 kV; resolution, 1500) coupled to a DS 90 data system. The atom gun was an adapted saddle field source (Ion Tech Ltd) operated at *ca.* 7 keV with a tube current of *ca.* 2 mA. Xenon was used to provide a primary beam of atoms and the sample $\mathbf{3}\cdot 4PF_6$ was dissolved in a small volume of 3-nitrobenzyl alcohol, which had previously been coated onto a stainless-steel probe tip. Spectra were recorded in the positive-ion mode at a scan speed of 30 s per decade.

‡ *Crystal data* for $\mathbf{3}\cdot 4PF_6$: $C_{78}H_{85}F_{24}N_7O_{10}P_4$, M = 1860.4, triclinic, a = 10.907(3), b = 13.899(5), c = 28.240(8) Å, α = 80.01(3), β = 85.89(2), γ = 89.72(3)°, U = 4205 Å^3, space group $P\bar{1}$, Z = 2, D_c = 1.47 g cm^{-3}, μ = 18 cm^{-1}. Data were measured on a Nicolet R3m diffractometer with Cu-Kα radiation (graphite monochromator) using ω-scans. The structure was solved by direct methods and refined anisotropically to give R = 0.127, R_w = 0.111 for 4635 independent reflections [$|F_0| > 3\sigma(|F_0|)$, $2\theta \leqslant 100°$]. Atomic coordinates, bond lengths and angles, and thermal parameters have been deposited at the Cambridge Crystallographic Data Centre. See Notice to Authors. Issue No. 1.

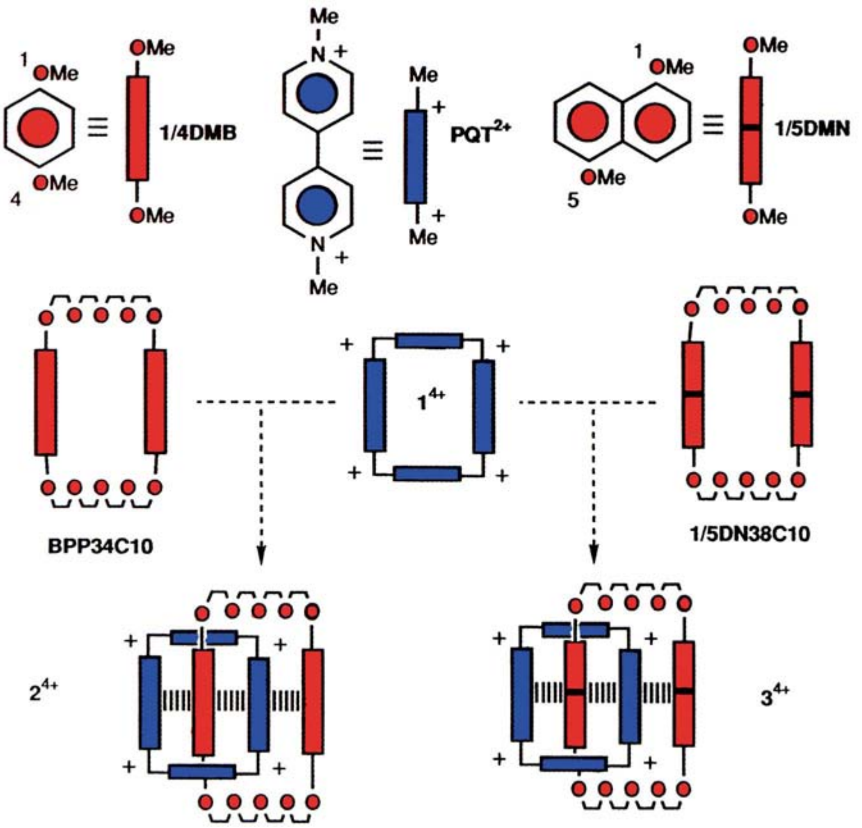

Fig. 1 Defining the chemical cartoons for the molecular components 1^{4+}, BPP34C10 and 1/5DN38C10 implicated in the construction of the [2]catenanes 2^{4+} and 3^{4+}. *p*-Phenylene rings ≡ small blue rectangles. Bipyridinium rings ≡ large blue rectangles. 1,4-Dioxybenzene rings ⊟ red rectangles. 1,5-Dioxynaphthalene rings ⊟ dissected red rectangles.

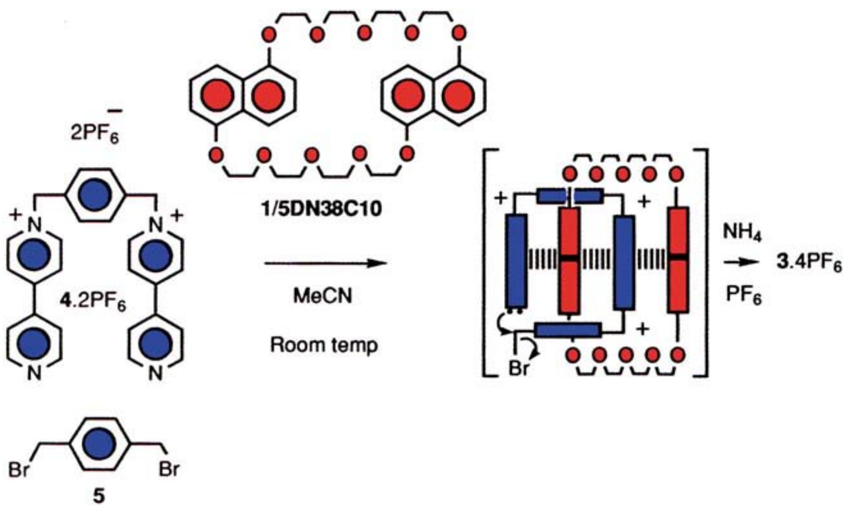

Scheme 1 The template-directed synthesis of the [2]catenane $3{\cdot}4PF_6$. Donor and acceptor macrocycles are red and blue, respectively.

ium units§ of the tetracationic macrocycle,[3,4] whilst the other residue lies outside and immediately adjacent to one of these bipyridinium units. The near parallel alignments of all four aromatic rings, coupled with a substantial degree of overlap (Fig. 3) in the donor–acceptor array, indicate the presence of strong π–π interactions[8] that are undoubtedly an important component in the stabilisation of this molecular assembly. The mean interplanar separations within this assembly are in the range 3.4–3.5 Å. An additional and notable interaction in this case is a very strong aromatic–aromatic edge-to-face interac-

---

§ The tetracationic macrocycle in 3^{4+} displays typical 'barrel-like' distortions. The strain within the cyclophane structure is relieved by out-of-plane bending of the six aromatic rings and is distributed throughout the macrocycle with the maximum deviations associated with the exocyclic C–CH$_2$ bonds emanating from the paraphenylene residues. These bonds subtend angles of 12° and 13° with respect to each other, whilst the $^+$N–CH$_2$ bonds associated with the bipyridinium units subtend angles of 19° and 22°. There are also concomitant reductions in the macrocyclic valency angles (105°–107°) at each of the four methylene bridges.

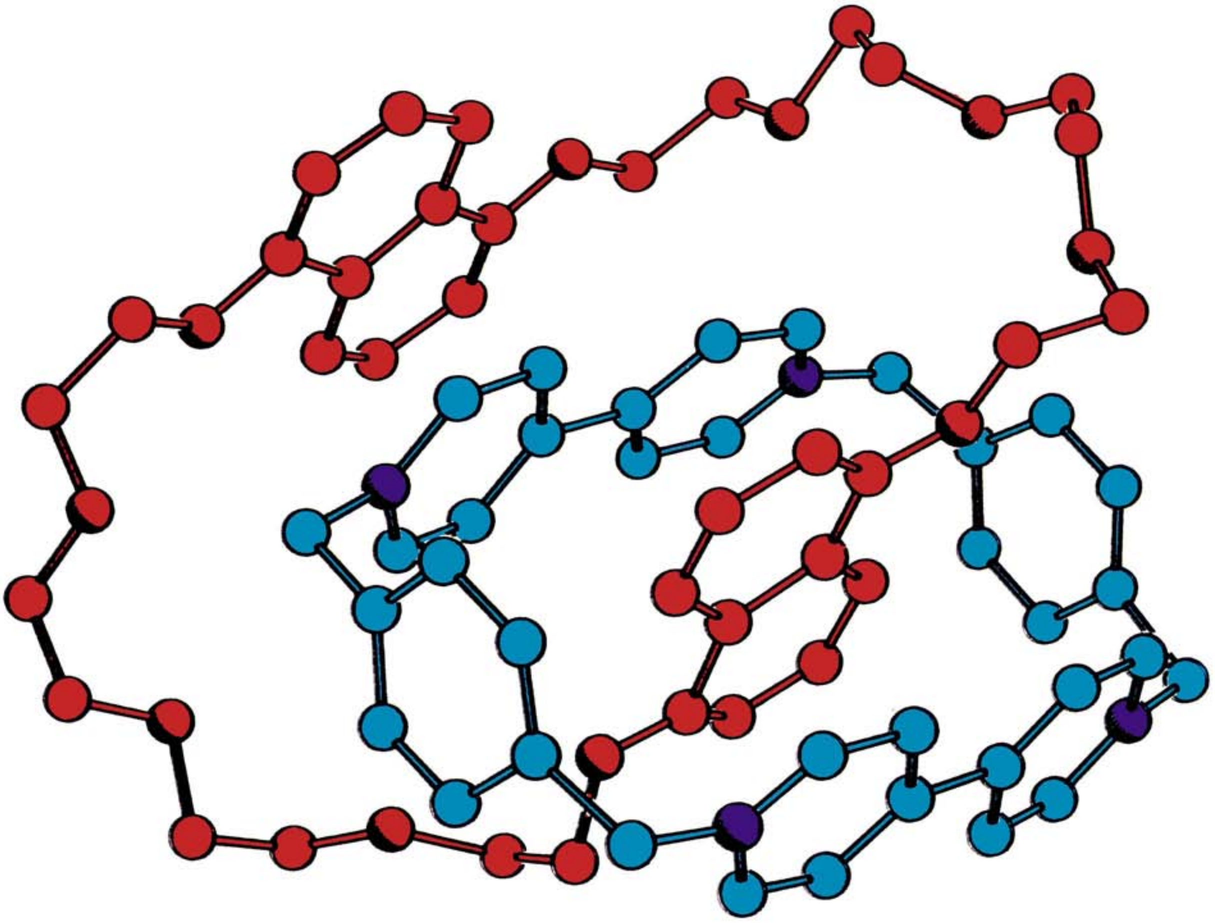

Fig. 2 Structure of 3^{4+} in the crystal with donor and acceptor macrocycles shaded red and blue, respectively. O atoms are dark red and N atoms are dark blue.

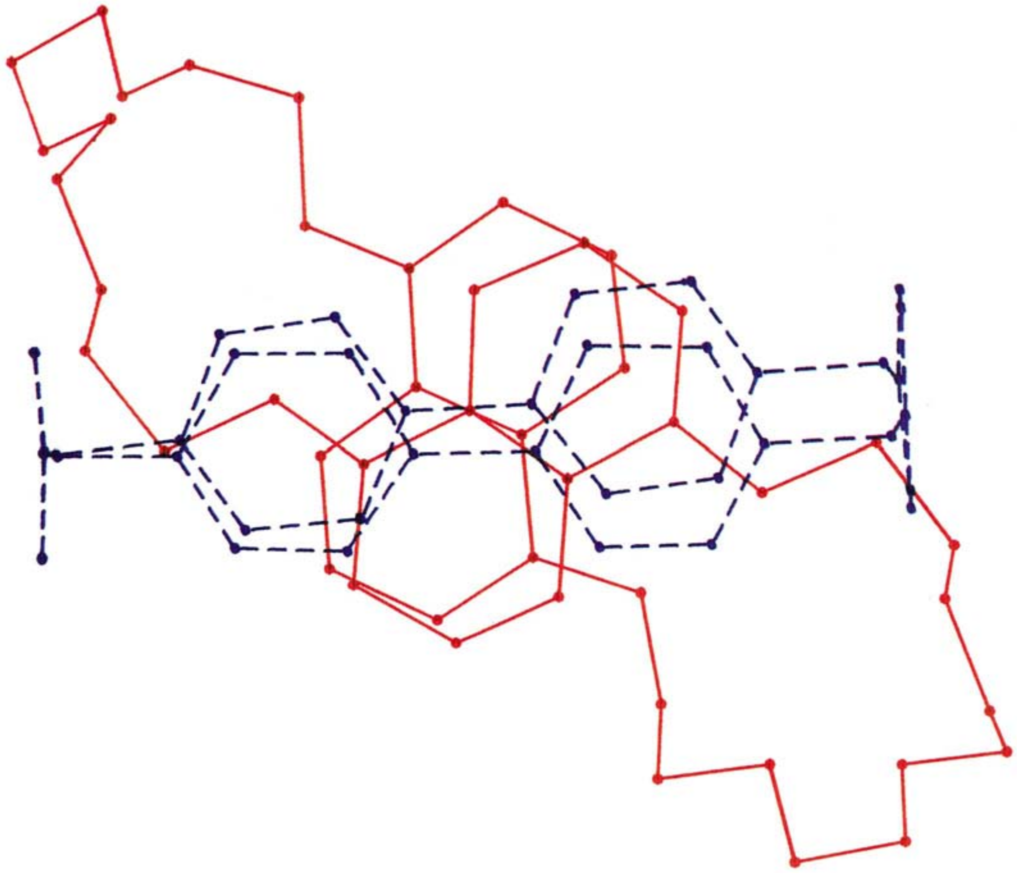

Fig. 3 Skeletal representation of 3^{4+} viewed normal to the plane of the 1,5-dioxynaphthalene ring lying within the tetracationic cavity. The donor is red and the acceptor is blue.

tion[9,10] between the included naphtho residue rings[§] (centroid–centroid separations of 4.7 and 4.8 Å) with both H-4 and H-8 of the naphtho residue directed orthogonally into the centres of the paraphenylene rings of the tetracationic macrocycle. Furthermore, as in the [2]catenane $\mathbf{2}^{4+}$, the molecules of $\mathbf{3}^{4+}$ are arranged in the crystal to form a continuous π-donor/π-acceptor stack (Fig. 4) with the 'alongside' bipyridinium unit of one catenane separated by a mean interplanar separation of only 3.3 Å from the 'alongside' 1,5-dinaphtho unit of the next.

The temperature dependent behaviour of the ^{1}H NMR spectrum of $\mathbf{3}^{4+}$ in solutions of CD_3COCD_3 and/or CD_3CN, covering the range from −80 to +80 °C, reveals the existence of a surfeit of site exchange processes arising from three discrete degenerate structural changes overcoming barriers associated with three different energies of activation. ^{1}H NMR spectroscopic data, obtained[¶] at −60, +40 and +80 °C, allow the following conclusions to be drawn with reference to a preferred structure (Fig. 5) in solution that is not dissimilar in its gross structural features from the solid state one (Fig. 2). At −60 °C, all the major structural changes, which can occur within the [2]catenane, are slow on the ^{1}H NMR time-scale. This situation is reflected in the observation of six signals for the symmetry-related pairs of protons H-2/6, H-3/7 and H-4/8 on the 'inside' and 'alongside' 1,5-naphtho rings, which impose their local twofold symmetry upon both the 'inside' and 'alongside' bipyridinium rings such that a total of eight signals are observed for the pairs of α, α′, β and β′ protons on

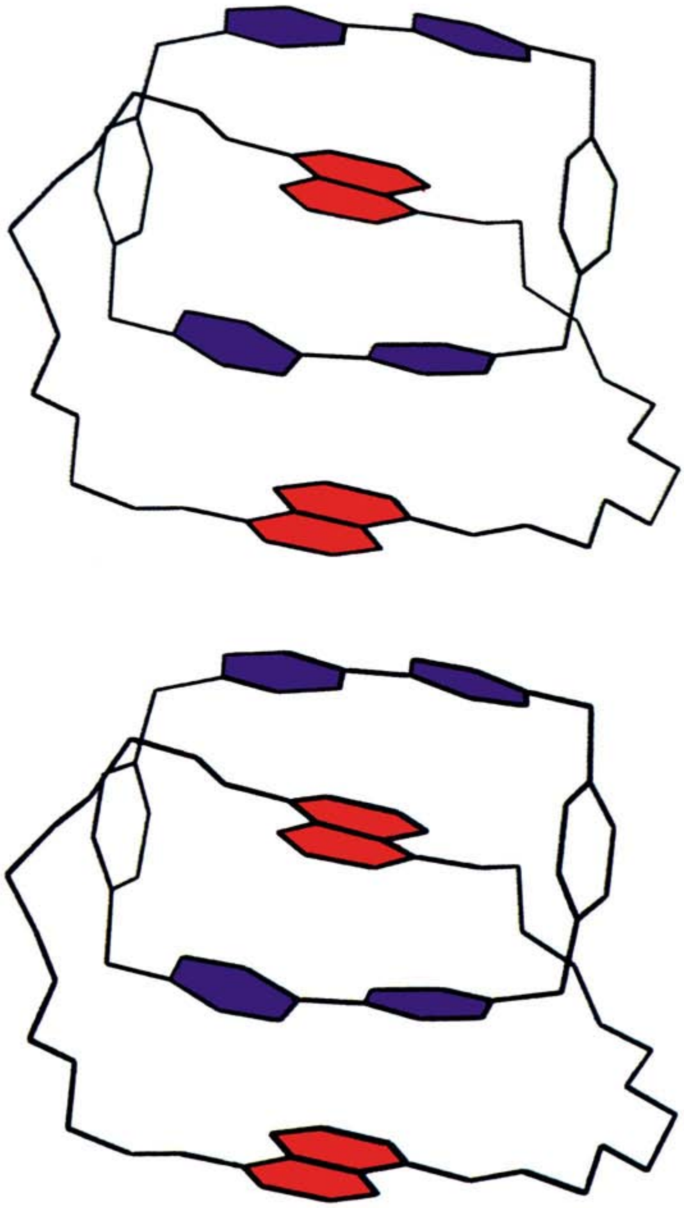

Fig. 4 Part of the continuous sequence of [2]catenanes $\mathbf{3}^{4+}$ in the crystal. Donors are red and acceptors are blue.

[¶] ^{1}H NMR data for $\mathbf{3}\cdot 4PF_6$ at −60 °C (400 MHz in CD_3COCD_3 containing 5% CD_3CN): δ 2.43 (2H, d, 'inside' H-4/8), 3.68–3.87 (12H, m, OCH_2), 3.91–4.02 (6H, m, OCH_2), 4.10–4.22 (6H, m, OCH_2), 4.22–4.30 (4H, m, OCH_2), 4.38–4.46 (4H, m, OCH_2), 5.90–6.04 (6H, m, $^+NCH_2$), 5.99 (2H, t, 'inside' H-3/7), 6.13 (2H, d, $^+NCH_2$), 6.14 (2H, d, 'inside' H-2/6), 6.33 (2H, d, 'alongside' H-2/6), 6.99 and 7.21 (2 × 2H, m, C_6H_4), 7.01 (2H, t, 'alongside' H-3/7), 7.11 (2H, d, 'alongside' H-4/8), 7.67 (4H, m, C_6H_4), 8.07, 8.12, 8.28 and 8.33 (4 × 2H, 4 × d, 'inside' and 'alongside' β and β′ bipy CH), and 8.71, 9.03, 9.10 and 9.30 (4 × 2H, 4 × d, 'inside' and 'alongside' α and α′ bipy CH). ^{1}H NMR data for $\mathbf{3}\cdot 4PF_6$ at +40 °C (400 MHz in CD_3CN): δ 2.31 (2H, d, 'inside' H-4/8), 3.68–3.72 (4H, bm, αOCH_2), 3.76–3.79 (4H, bm, βOCH_2), 3.79–3.82 (4H, bm, γOCH_2), 3.89–3.94 (4H, bm, δOCH_2), 3.96–4.01 (4H, bm, $\delta' OCH_2$), 4.02–4.06 (4H, bm, $\gamma' OCH_2$), 4.08–4.12 (4H, bm, $\beta' OCH_2$), 4.21–4.24 (4H, bm, $\alpha' OCH_2$), 5.63 (4H, d, $^+NCH_2$), 5.82 (2H, t, 'inside' H-3/7), 5.84 (4H, d, $^+NCH_2$), 6.09 (2H, d, 'inside' H-2/6), 6.36 (2H, d, 'alongside' H-2/6), 6.88 (8H, bd, 2 × C_6H_4), 7.12 (2H, t, 'alongside' H-3/7), 7.18 (2H, d, 'alongside' H-4/8), 7.88 and 8.04 (2 × 4H, bs, β and β′ bipy CH), and 8.39 and 8.86 (2 × 4H, d, α and α′ bipy CH). ^{1}H NMR data for $\mathbf{3}\cdot 4PF_6$ at +80 °C (400 MHz in CD_3CN): δ 2.27–2.60 (2H, bm, 'inside' H-4/8), 3.55–4.49 (32H, bm, α/α′/β/β′/γ/γ′/δ/δ′ OCH_2), 5.53–6.00 (10H, bm, 4 × $^+NCH_2$ and 'inside' H-3/7), 6.10–6.50 (4H, bm, 'inside' and 'outside' H-2/6), 7.03–7.35 (4H, bm, 'outside' H-3/7 and H-4/8), 6.91 (8H, m, 2 × C_6H_4), 7.99 (8H, bm, β/β′ bipy CH), and 8.30–9.00 (8H, bm, α/α′ bipy CH).

Decoupling difference experiments carried out at −60 °C were used to identify the resonances in the ^{1}H NMR spectrum arising from the 'inside' and 'alongside' 1,5-naphtho units with respect to the cavity of $\mathbf{1}^{4+}$, after the 'inside' H-4/8 protons had been assigned to the high field signal resonating at δ 2.43. The fact that this signal is moved dramatically upfield by 4.68 ppm relative to the chemical shift of the 'alongside' H-4/8 protons reflects the fact that these two protons are very much under the shielding influence of the aromatic rings in the tetracation. Using the equivalent dipole model (R. J. Abraham, S. C. M. Fell and K. M. Smith, *Org. Magn. Reson.*, 1977, **9**, 367) of an aromatic ring, it is possible to calculate the shielding effect (Δδ) experienced by protons placed above the plane of the aromatic ring. Using the equation, $\Delta\delta = k(1 - 3\cos^2\alpha)/r^3$, where k is a constant, r is the distance (in Å) from the centroid of the aromatic ring to the probe proton and α is the angle subtended to the normal to the plane of the aromatic ring by the probe proton–centroid vector, Δδ values can be calculated. For the 'inside' H-3/7 and H-4/8 protons, Δδ (calcd.) values of 0.99 and 4.65 ppm were computed when appropriate values of k (14.1 for the pyridinium rings and 27.6 for the *p*-xylylene residue) were employed along with the values for α and r obtained from the X-ray crystal structure. The fact that the Δδ (calcd.) values are very close to the Δδ (exptl.) values of 1.02 and 4.68 ppm, respectively, for the 'inside' H-3/7 and H-4/8 protons suggests that there is a very close correspondence between the solution and solid state structures of $\mathbf{3}^{4+}$, at least in the central region of the tetracationic cavity of the [2]catenane.

The OCH_2 groups in the polyether chains were assigned to the eight signals observed in the ^{1}H NMR spectrum at +40 °C by employing, first of all, NOE difference experiments to identify the α OCH_2 group by irradiating the H-2/6 signal on the 'inside' naphtho unit, and then subsequently decoupling difference experiments to establish that the sequence of OCH_2 units is α, β, γ, δ, δ′, γ′, β′ and α′ as the progression is made from high to low field.

In the analysis of the temperature dependent ^{1}H NMR spectra, both the coalescence (I. O. Sutherland, *Ann. Rep. NMR Spectrosc.*, 1971, **4**, 71) and the exchange (J. Sandström, *Dynamic NMR Spectroscopy*, Academic Press, London, 1982, ch. 6) methods were employed. In the coalescence method, values of k_c were obtained using the approximate expression $k_c = \pi(\Delta\nu)/(2)^{1/2}$ and the Eyring equation was then used to calculate $\Delta G_c^{\ddagger}$ values at T_c. In the exchange method, values of k were obtained using the approximate expression $k = \pi(\Delta\nu)$ and again the Eyring equation was used to calculate $\Delta G^{\ddagger}$ values at T.

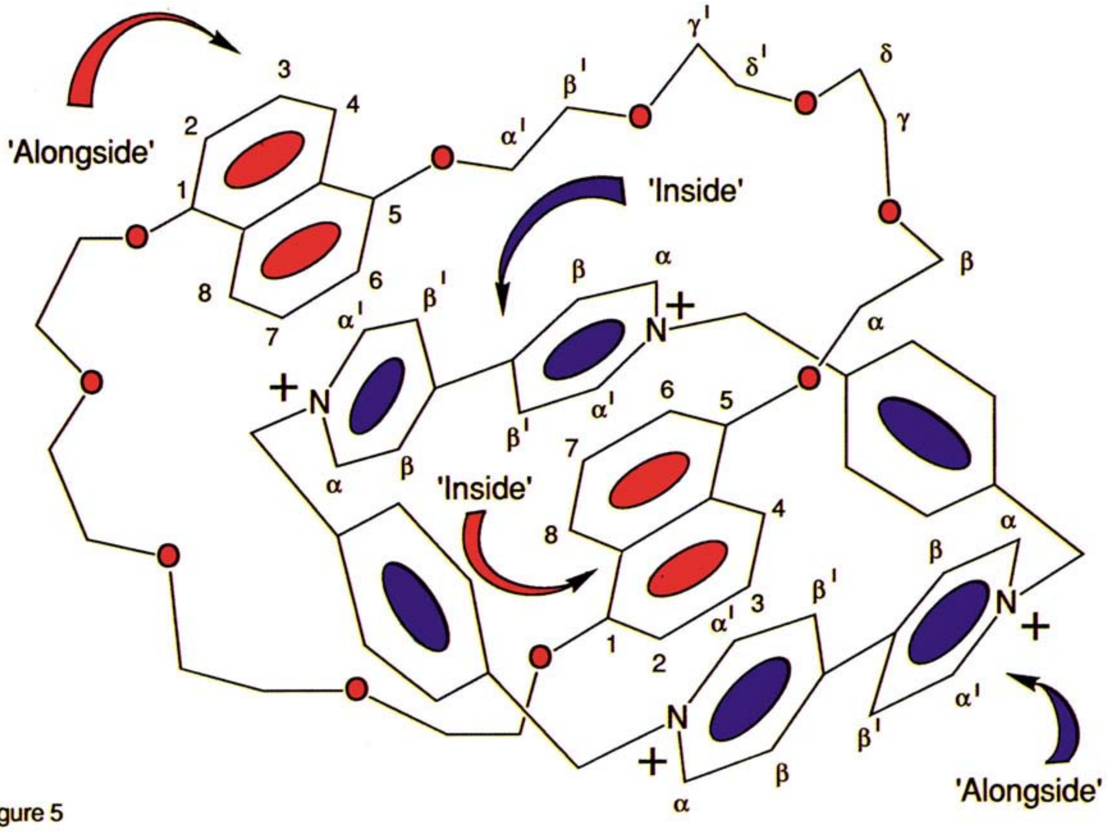

Figure 5

Fig. 5 The preferred structure of 3^{4+} in solution with descriptors that aid in the discussion of the temperature dependent ^{1}H NMR spectra. The donor and acceptor macrocycles are shaded red and blue, respectively.

each bipyridinium ring. It is also transparent that, in keeping with the symmetry considerations, both the benzylic $^{+}NCH_2$ protons and the paraphenylene ring protons give rise to four signals each at −60 °C. The signal pattern for the 16 heterotopic OCH_2 protons in each equivalent polyether chain is necessarily a complicated one which simplifies most elegantly at +40 °C to eight signals for the α, β, γ, δ, δ′, γ′, β′ and α′ OCH_2 protons. At this temperature, the 'alongside' 1,5-naphtho residue in the 1/5DN38C10 component is pirouetting around the periphery of the tetracationic component with the consequence that, although the 1,5-naphtho rings in 'inside' and 'alongside' environments maintain their identities and still give rise to six signals, the number of resolved resonances for bipyridinium ring protons is reduced from eight to four signals, indicating the loss of their 'inside' and 'alongside' distinctions, but requiring the retention of the difference between the α, α′, β and β′ protons imposed by the local twofold symmetries of the 1,5-naphtho rings. A $\Delta G^{\ddagger}$ value‖ of 12.7 kcal mol^{-1} for the revolving motion undergone by 1/5DN38C10 that exchanges 'inside' and 'alongside' bipyridinium rings in 1^{4+} was estimated from the rate constant (k 75 s^{-1}) calculated on the basis of the line broadening ($\Delta\nu$ = 24 Hz) experienced by the α or α′ bipyridinium ring proton resonance at δ 8.71 when the temperature, T, of the CD_3COCD_3–CD_3CN (19:1) solution is −16 °C. Above +40 °C, the signals for the α and α′, and β and β′, bipyridinium ring protons coalesce to two signals as site exchanges involving the constitutionally identical bipyridinium ring protons occur more rapidly on the ^{1}H NMR time-scale. For the signal which emerges at δ 7.99 (at +80 °C), after having coalesced at +52 °C from individual signals for the β and β′ bipyridinium ring protons that are separated by 63 Hz in the chemical shift limit ($\Delta\nu_c$), a rate constant (k_c 140 s^{-1}) is calculated from which a $\Delta G_c^{\ddagger}$ value of 15.8 kcal mol^{-1} follows. This free energy barrier can be interpreted as the one required to dislodge the 'inside' 1,5-naphtho unit from within the cavity of 1^{4+} such that the 1,5-naphtho unit can reorientate itself before it re-enters the cavity. The net result of this 'out, turn around, and in again' process is the eradication of the influence of the local twofold symmetry of the 1,5-naphtho units upon the tetracationic portion of the [2]catenane. When the temperature of a CD_3CN solution of $3\cdot4PF_6$ reaches +80 °C, all the protons in the molecule that can, in principle, undergo site exchange are doing so on the ^{1}H NMR time-scale. In particular, the three pairs of signals for the constitutionally identical 1,5-naptho protons, *i.e.* H-2/6, H-3/7 and H-4/8, coalesce to three signals as the 'inside' and 'alongside' environments of the 1,5-naphtho rings are equilibrated as a result of the 1/5DN38C10 ring threading its way freely through the cavity of 1^{4+}. Relying on H-2/6 as a probe, two signals, separated in the chemical shift limit ($\Delta\nu$) by 108 Hz, coalesce at +86 °C, giving a rate constant (k_c 240 s^{-1}) from which a $\Delta G_c^{\ddagger}$ value‖ of 17.2 kcal mol^{-1} is obtained. Thus, we conclude that, even in solution, the [2]catenane 3^{4+} is a highly ordered molecular assembly.

‖ These free energy barriers of 12.7 and 17.2 kcal mol^{-1} obtained from dynamic ^{1}H NMR spectroscopic investigations on 3^{4+} can be compared (ref. 6) with those of 12.2 and 15.6 kcal mol^{-1} for the analogous degenerate structural changes in 2^{4+}. Obviously, when the aromatic rings in the macrocyclic polyether are 1,5-naphtho units rather than hydroquinol residues, there is little or no difference in the demands placed upon the macrocyclic polyether revolving around the tetracationic cyclophane. However, when the macrocyclic polyether is feeding itself through the tetracationic cyclophane, the process is clearly somewhat more demanding when the aromatic rings in the macrocyclic polyether are 1,5-naphtho units rather than hydroquinol residues.

Table 1 The potential and thermodynamic parameters for the electrochemical reductions[a] of **1**·4PF$_6$, **2**·4PF$_6$ and **3**·4PF$_6$

Compound	E_1^0/mV	$E_1^{0'}$/mV	E_2^0/mV	Half-width ($E_p - E_{p/2}$)/mV	$\Delta E_{1/2}$/mV	K_c
1·4PF$_6$	−283	—	−708	59.7[b]	40.2[b]	4.8[b]
2·4PF$_6$	−310	−437	−845	180.6[b]	148.9[b]	329.0[b]
3·4PF$_6$	−354	−572	−861	250.0[b]	210.0[b]	3548.9[b]

[a] Electrochemical experiments were performed with a Princeton Applied Research Model 175 universal programmer, a Model 173 potentiostat, and a Model 179 digital coulometer equipped with positive feedback circuitry for IR compensation. Voltammograms were recorded on a Soltex VP-6423S X-Y recorder. A glassy carbon disk electrode (0.080 cm^2), Pt flag, and sodium chloride saturated calomel electrode (SSCE) were used as the working, auxiliary and reference electrodes, respectively. All solutions for the voltammetric experiments were deoxygenated by sparging with nitrogen gas; a nitrogen atmosphere was maintained above the solution during the experiments. [b] The half-width (E_p–$E_{p/2}$/mV) values were measured on the first reduction peak of the voltammogram. Following a literature procedure (D. E. Richardson and H. Taube, *Inorg. Chem.*, 1981, **20**, 1278), these values were used to calculate the actual difference ($\Delta E_{1/2}$ mV) between the two PQT^{2+}/PQT$^+$ half-wave potentials, and K_c, the equilibrium conproportionation constant for the process $X^{2+} + X^{4+} = 2X^{3+}$ where X may be any of the bis(bipyridinium) compounds, from the expression, $K_c = \exp[(\Delta E_{1/2})F/RT]$.

Cyclic voltammetry of **3**·4PF$_6$ in MeCN–Bu$_4$NPF$_6$ (0.1 mol dm^{-3}) shows (Table 1) three reversible reduction processes with half-wave potentials of −354, −572 and −861 mV *vs.* SSCE. The first two processes are monoelectronic reductions corresponding to the PQT^{2+}/PQT$^+$ couples, while the third one is a two electron reduction corresponding to the almost simultaneous PQT$^+$/PQT conversion of both subunits. The redox behaviour is qualitatively similar (Table 1) to that[5] of **2**·4PF$_6$ and results from the topological differences between the 'alongside' and 'inside' bipyridinium units. In both [2]catenanes, the latter PQT^{2+} group is substantially stabilized by charge transfer interactions with two aromatic donor units, and, therefore, undergoes reduction to the PQT$^+$ form at more negative potentials than the 'alongside' PQT^{2+} group. The topological differences between the bipyridinium groups exert a much smaller effect on the PQT$^+$/PQT couples because of the diminished acceptor character of these bipyridinium oxidation states. The difference between the 'alongside' and 'inside' PQT^{2+}/PQT$^+$ half-wave potentials is larger for **3**$^{4+}$ (218 mV) than for **2**$^{4+}$ (149 mV) revealing that the relative stabilization of the 'inside' PQT^{2+} subunit is greater in the former [2]catenane.

The syntheses of the [2]catenanes **2**$^{4+}$ and **3**$^{4+}$ provide excellent examples in chemical systems of self-assembly in the first steps of the syntheses with post-assembly modification—as a result of covalent bond formation—in the second steps. The fact that these particular compounds can be made to order with such relative ease augurs well for the design and construction of more intricate and highly structured molecular assemblies with physical properties that could become increasingly intriguing.

We acknowledge financial support from AFRC, SERC, NEDO, ICI, the Leverhulme Trust and the University of Miami.

Received, 4th February 1991; Com. 1/00517K

References

1 J.-Y. Ortholand, A. M. Z. Slawin, N. Spencer, J. F. Stoddart and D. J. Williams, *Angew. Chem., Int. Ed. Engl.*, 1989, **28**, 1394.
2 M. V. Reddington, A. M. Z. Slawin, N. Spencer, J. F. Stoddart, C. Vicent and D. J. Williams, *J. Chem. Soc., Chem. Commun.*, 1991, preceding communication.
3 B. Odell, M. V. Reddington, A. M. Z. Slawin, N. Spencer, J. F. Stoddart and D. J. Williams, *Angew. Chem., Int. Ed. Engl.*, 1988, **27**, 1547.
4 P. R. Ashton, B. Odell, M. V. Reddington, A. M. Z. Slawin, J. F. Stoddart and D. J. Williams, *Angew. Chem., Int. Ed. Engl.*, 1988, **27**, 1550.
5 P. R. Ashton, T. T. Goodnow, A. E. Kaifer, M. V. Reddington, A. M. Z. Slawin, N. Spencer, J. F. Stoddart, C. Vicent and D. J. Williams, *Angew. Chem., Int. Ed. Engl.*, 1989, **28**, 1396.
6 P. L. Anelli, P. R. Ashton, R. Ballardini, V. Balzani, M. Delgado, M. T. Gandolfi, T. T. Goodnow, A. E. Kaifer, D. Philp, M. Pietraszkiewicz, L. Prodi, M. V. Reddington, A. M. Z. Slawin, N. Spencer, C. Vicent and D. J. Williams, *J. Am. Chem. Soc.*, submitted for publication.
7 W. Geuder, S. Hünig and A. Suchy, *Angew. Chem., Int. Ed. Engl.*, 1983, **22**, 489; *Tetrahedron*, 1986, **42**, 1665.
8 C. A. Hunter and J. K. M. Sanders, *J. Am. Chem. Soc.*, 1990, **112**, 5525, and references cited therein.
9 S. K. Burley and G. A. Petsko, *Adv. Protein Chem.*, 1988, **39**, 125, and references cited therein.
10 W. L. Jorgensen and D. L. Severance, *J. Am. Chem. Soc.*, 1990, **112**, 4768, and references cited therein.